Bioorganic & Medicinal Chemistry Letters 19 (2009) 4622–4625

Contents lists available at ScienceDirect

Bioorganic & Medicinal Chemistry Letters

journal homepage: www.elsevier.com/locate/bmcl

Design of selective Cathepsin inhibitors

Paul A. Bethel [a], Stefan Gerhardt [a], Emma V. Jones [a], Peter W. Kenny [a,*], Galith I. Karoutchi [a], Andrew D. Morley [a,*], Keith Oldham [a], Neil Rankine [a], Martin Augustin [b], Stephan Krapp [b], Hannes Simader [b], Stefan Steinbacher [b]

[a] RIRA, AstraZeneca, Mereside, Alderley Park, Macclesfield, SK10 4TG, UK
[b] Proteros Biostructures, Am Klopferspitz 19, D-82152 Martinsried, Germany

ARTICLE INFO

Article history:
Received 30 April 2009
Revised 20 June 2009
Accepted 23 June 2009
Available online 27 June 2009

Keywords:
Cathepsin
Cathepsin B
Cathepsin K
Cathepsin L
Cathepsin L2
Cathepsin S
Cathepsin V
Cysteine protease
Nitrile
Covalent inhibitor
Selectity
Protein structure
X-ray crystallography
Structure-based design
Hydrogen bonding
Hot spot
Electrostatic
Hydrogen bond

ABSTRACT

A number of molecular recognition features have been exploited in structure-based design of selective Cathepsin inhibitors.

Cysteine Cathepsins are implicated in a number of diseases including cancer, osteoarthritis, osteoporosis, autoimmune disorders and viral infection.[1] Selectivity is an important consideration in design of inhibitors of this class of protease, especially given that many of these feature an electrophilic warhead, such as a nitrile, that interacts covalently with the active site cysteine. For instance, gene knockout studies suggest that Cathepsins B (CatB) and L2 (CatL2) should be considered key anti-targets in optimization of Cathepsin L (CatL) inhibitors.[2–4]

Compounds **1–3** were described recently as CatL inhibitors and the binding mode of **2** has been characterized by X-ray crystallography.[4] Interaction with Leu69 appears to be a factor in the improved selectivity profiles of **2** and **3** over **1**. The equivalent residue in a number of the other Cathepsins is an aromatic amino acid. This selectivity was unexpected at the outset because the molecular surface in the region of the Leu69 side chain is convex. One rationale for observed selectivity is that Leu69 interacts with a concave region of the ligand and is held in what we have described[4] as a 'molecular pincer'.

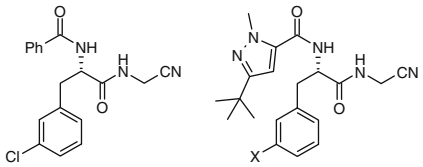

1 **2** : X = Me **3** : X = Cl

* Corresponding authors. Tel.: +44 1625 514396 (P.W.K.).
E-mail addresses: pwk.pub.2008@gmail.com (P.W. Kenny), andy.morley@astrazeneca.com (A.D. Morley).

0960-894X/$ - see front matter © 2009 Elsevier Ltd. All rights reserved.
doi:10.1016/j.bmcl.2009.06.090

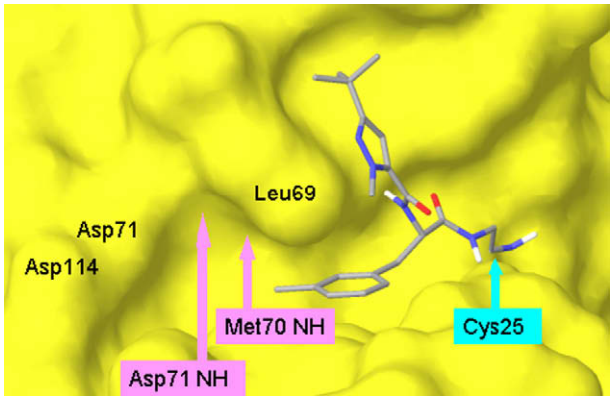

Figure 1. Crystal structure of **2** bound to Cathepsin L showing molecular surface of the protein and the locations of key residues.

Other residues that might be targeted to improve selectivity are Asp71 and Asp114. The corresponding residues in CatL2 are hydrophobic amino acids (Ala71; Val114). The crystal structure of **2** bound to CatL (Fig. 1) shows the side chains of Asp71 and Asp114 to be in mutual contact, suggesting that at least one of these residues is protonated under crystallization conditions. Provided that one of these aspartates remains anionic, achieving contact between this region of the protein and a cationic group in an inhibitor is likely to result in improved selectivity over CatL2.

It is important that the spacer that links this cationic group to the rest of the molecule makes contact with the surface of the protein. The backbone amide hydrogen bond donors of Met70 and Asp71 are of particular interest in this regard. These molecular recognition elements sit next to each other at the bottom of a pocket where the molecular surface of the protein is concave. Surface concavity[5] and solvent enclosure[6] in a binding pocket facilitate displacement of water molecules by ligand. These characteristics suggest that this region of the protein may be able to function as a hot spot[7,8] for ligand recognition. The presence of exposed polar atoms deep within a binding pocket contributes to the druggability[9] of a target protein especially when fragment-based approaches[10,11] are used. Exploiting these two hydrogen bond donors was seen as a means to anchor ligands in order to make more effective contact with the Asp71 and Asp114 residues. This approach was predicted to generate good selectivity with respect to CatB as the amino acid corresponding to Met70 is proline, which lacks a backbone donor.

The amide donors of Met70 and Asp71 reinforce each other because they are close together and mutually aligned.[12,13] An adjacent pair of hydrogen bond acceptor nitrogen atoms in a heteroaromatic ring is a molecular recognition feature that is highly complementary to the aligned donors. Repulsion between the aligned nitrogen lone pairs enhances the hydrogen bond acceptor strength of each nitrogen atom.[13–15] Inspection of the crystal structure for the complex of **2** and CatL suggested that linking from C3 of the phenyl ring would provide the best access to the amide donors. A number of analogs of **2**, C3-substituted with heteroaromatic rings, were synthesized.

The esters **5** were prepared from commercially available 3-bromophenylalanine (**4**). Subsequent hydrolysis followed by amide coupling with aminoacetonitrile generated the key 3-bromophenylalanine derivatives **6** (Scheme 1). Compounds **7–13** and **15** were prepared in low to moderate yield by Suzuki coupling with various commercially available heterocyclic boronic acid pinacol esters. Protecting groups were present in two of these reagents and these were removed using standard methods to give **14** and **16**.

The boronic acid/esters required for synthesis of **20–22** using the route described in Scheme 1 were not readily available. These compounds were prepared via Suzuki coupling of the commercially available heteroaryl triflates/bromides with the boronic acid pinacol ester **19** (Scheme 2). This racemic intermediate was obtained from **17** by conversion to triflate **18** followed by cross-coupling reaction with bis(pinacolato)diboron.

Compound **23** was prepared as previously described from commercially available (*S*)-*m*-tyrosine. Subsequent conversion to triflate followed by hydroxycarbonylation using molybdenum hexacarbonyl generated the key acid intermediates **24**. Standard HATU coupling with various hydrazides either commercially available (or prepared) followed by cyclodehydration with either Burgess reagent or Lawesson's reagent afforded oxadiazoles/thiazdiazoles **25**. Subsequent ester hydrolysis followed by amide coupling with aminoacetonitrile generated **26–32**. Demethylation of compound **25a** with boron tribromide, followed by hydrolysis and amide formation afforded **33**. Formic acid mediated Boc deprotection of intermediates **34** and **36** afforded compounds **35** and **37** (Scheme 3).

Cathepsin inhibition profiles are presented in Table 1 for a number of phenylalanine derivatives with heteroaromatic substituents at C3. Compounds with 3-pyridazinyl (**21**) 1,3,4-oxadiazolyl (**26**, **28**), or 1,3,4-thiadiazolyl (**27**, **29**) substituents at C3 were consistently more potent than the corresponding 3-chloro analogues (**1**, **3**) against CatS and CatL2. Compounds **21** and **27** are particularly potent CatS inhibitors with good selectivity over other family members, and would be useful start points for a program against this target.[19]

Different trends were observed for CatL potency and the presence of adjacent hydrogen bond acceptors appears to less beneficial than for CatS or CatL2. For example, the CatL pIC_{50} of **21** is 0.7 units less than that of **1** and **29** is slightly more potent (0.4 units) than **3** against CatL. This suggests that Leu69 may restrict

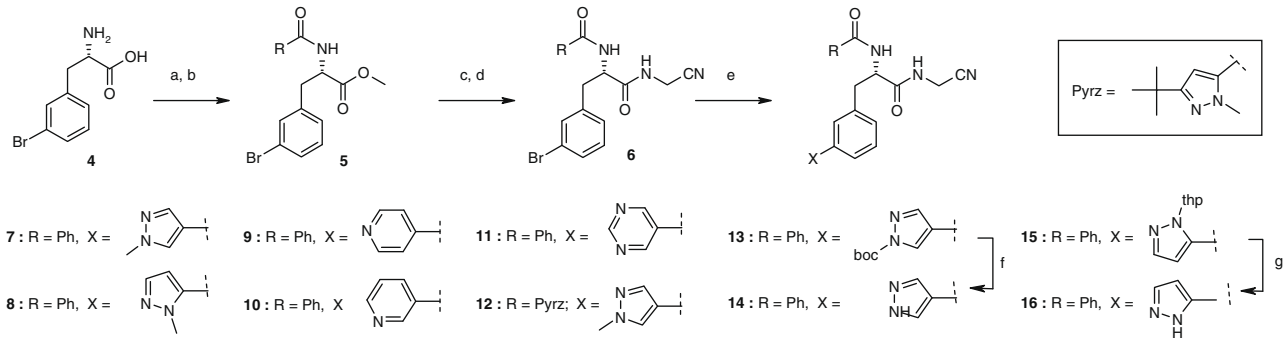

Scheme 1. Reagents and conditions: (a) 10 M HCl/MeOH; (b) acid, HATU, DIPEA, DMF; (c) LiOH, MeOH/H_2O/THF; (d) H_2NCH_2CN, HATU, DIPEA, DMF; (e) het-boronic acid pinacol ester, 1,1 bis(di-*tert*-butylphospino)ferrocene palladium dichloride, Na_2CO_3, dioxane/H_2O, 100 °C, MW; (f) formic acid; (g) 1.25 M HCl/EtOH.

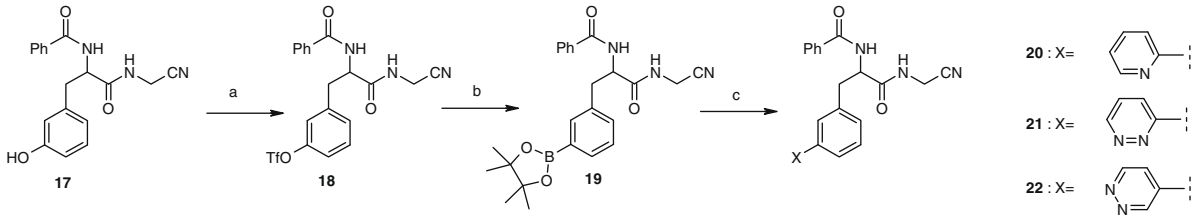

Scheme 2. Reagents and conditions: (a) $PhNTf_2$, K_2CO_3, THF, 120 °C, MW; (b) bis(pinacolato)diboron, 1,1 bis(di-*tert*-butylphospino)ferrocene palladium dichloride, KOAc, DME, 85 °C; (c) het-OTf/Br, $Pd(OAc)_2$, K_3PO_4, S-Phos, THF/H_2O, 150 °C, MW.

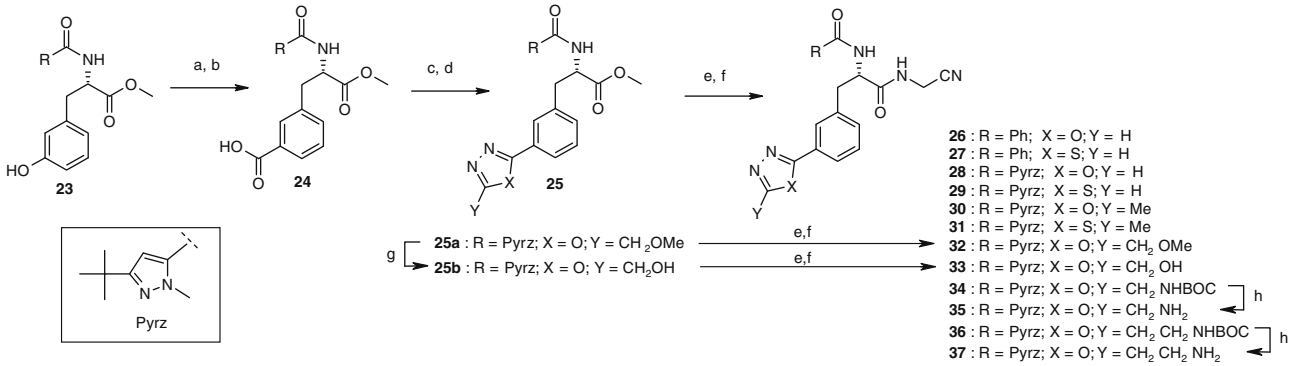

Scheme 3. Reagents and conditions: (a) $PhNTf_2$, K_2CO_3, THF, 120 °C, MW; (b) $Mo(CO)_6$, $Pd(OAc)_2$, dppf, K_2CO_3, dioxane, 140 °C, MW; (c) hydrazide, HATU, DIPEA, DCM, rt; (d) burgess reagent, 70 °C, MW or Lawesson's reagent, 40 °C, THF; (e) 2.5 N aq NaOH, $MeOH/H_2O$, 75 °C; (f) H_2NCH_2CN, HATU, DIPEA, DMF; (g) BBr_3, DCM, rt; (h) formic acid, rt.

interaction of the heterocyclic nitrogen atoms with the backbone donors to a greater extent than the corresponding Phe residues in CatS and CatL2. Subtle SAR was observed for these structural types. For example, **30** is 0.5 log units more potent than **28** against CatL but **31** is 1.4 log units less potent than **29**.

The methoxy (**32**) and hydroxyl (**33**) analogues of **30** showed inhibition profiles that were very similar to that observed for **30**. Compounds **35** and **37**, each of which presents a pendant amino group that is largely protonated under assay conditions, are 0.4 and 0.6 log units more potent than **30** against CatL. Both CatL2 and CatS potencies are lower for the cationic compounds than for **30**, resulting in better selectivity profiles. Compound **35** shows greater selectivity ($\Delta pIC_{50} = -2.0$) against CatS than CatL2 ($\Delta pIC_{50} = -1.3$). Compound **37** shows a better overall selectivity profile than **35** with a marginally greater bias against CatL2 ($\Delta pIC_{50} = -1.9$) than CatS ($\Delta pIC_{50} = -1.7$).

The crystal structure[20] of **35** bound to CatL shows contact between the cationic amino substituent and the interacting Asp71-Asp141 pair (Fig. 2). There are four protein molecules in the asymmetric unit and contact distances between oxadiazole nitrogen atoms and backbone amide hydrogen atoms lie in the range 2.21 Å to 2.52 Å for Met70 and 2.45 Å to 2.78 Å for Asp71. These hydrogen bonds are relatively long and the greater CatS potency of **21**, **26** and **27** may reflect hydrogen bond geometries that are closer to ideal values when these compounds are bound to CatS.

Table 1
Cathepsin pIC_{50} values

Compd	Cat L pIC_{50}[a]	Cat L2 pIC_{50}[a]	Cat B pIC_{50}[a]	Cat K pIC_{50}[a]	Cat S pIC_{50}[a]
1	6.6	6.1	5.3	5.5	6.9
2	7.9	6.4	5.4	5.6	6.1
3	7.9	6.7	5.2	5.5	6.0
7	6.3	5.8	5.2	<5	7.0
8	5.5	5.5	5.1	<5	6.5
9	5.8	5.5	<5	<5	6.6
10	5.7	5.4	5.1	<5.1	6.9
11	5.4	<5.1	<5	<5.1	6.5
12	7.8	6.8	<5	5.2	6.5
14	6.1	5.8	5.1	<5	7.1
16	5.8	5.4	5.3	<5	6.5
20	5.5	<5	5.2	<5	6.2
21	5.9	7.2	5.2	<5.2	8.1
22	<5.1	<5	<5	<5	6.1
26	6.3	6.8	<5	5.9	7.7
27	6.7	7.6	<5	6.2	8.6
28	7.8	7.7	<5	6.9	7.2
29	8.3	8.2	<5	6.9	7.8
30	8.3	8.2	<5	7.2	7.1
31	6.9	8.5	<5	5.5	6.5
32	8.4	8.7	<5	6.9	7.1
33	8.2	8.1	<5	7.0	7.2
35	8.7	7.4	5.4	6.0	6.7
37	8.9	7.0	5.2	6.8	7.2

[a] Values are means of at least three experiments; see Refs. 16–18.

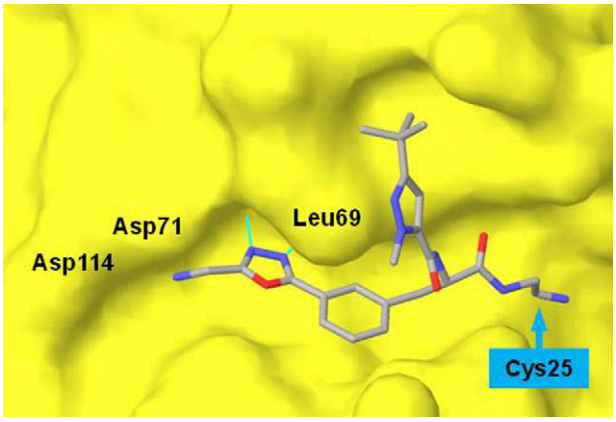

Figure 2. Crystal structure of **35** bound to Cathepsin L showing molecular surface of the protein and locations of key residues. The hydrogen bonds between the oxadiazole nitrogen acceptors and the backbone amide donors of Met70 and Asp71 are shown in turquoise.

This variability in the contributions of these hydrogen bonds to potency suggests that this region of the protein surface can be used to manipulate Cathepsin selectivity.

The CatS and CatL2 pIC_{50} values for **20** and **21** have implications beyond Cathepsin inhibition. Aza-substitution of **20** leading to **21**, which adds a hydrogen bond acceptor, leads to a 1.9 log unit increase in CatS potency. The CatL2 pIC_{50} difference for these compounds appears to be even larger (>2.2) although **20** is too weak an inhibitor to be detected in the assay. It has been suggested[23] that a neutral–neutral hydrogen bond can contribute no more than a factor of 15-fold (1.2 log units) to binding affinity. This is rather less than either of the differences in CatS (1.9) and CatL2 (>2.2) pIC_{50} values measured for **20** and **21** which suggests that the upper limit to the contribution of a neutral–neutral hydrogen bond to potency may be higher than was previously thought. Caution is needed when interpreting these results because **20** and **21** are both racemic and the structure of **21** bound to CatS is not currently available. However, the increase in potency resulting from isosteric introduction of a hydrogen bond acceptor into an inhibitor molecule is compelling evidence that the acceptor forms a hydrogen bond with the protein. It is also worth noting that while **21** is 0.7 units less potent than **1** against CatL it is still 0.4 units more potent than **20** against this enzyme.

In summary, we have exploited differences between protein structures to modulate Cathepsin selectivity. We have also demonstrated that an aligned pair of hydrogen bond donors can function as a hot spot. Finally we suggest that a proposed upper limit for the contribution of a neutral–neutral hydrogen bond is underestimated.

Acknowledgments

A number of pIC_{50} values were measured by Jack Dawson and Linda Wood. Lyn Rosenbrier Ribeiro and Helen Sawney shared assay development expertise.

References and notes

1. Vasiljeva, O.; Reinheckel, T.; Peters, C.; Turk, D.; Turk, V.; Turk, B. *Curr. Pharm. Des.* **2007**, *13*, 387.
2. Felbor, U.; Kessler, B.; Mothes, W.; Ploegh, H. L.; Goebel, H. H.; Bronson, R. T.; Olsen, B. R. *Proc. Nat. Acad. Sci.* **2002**, *99*, 7883.
3. Hagemann, S.; Günther, T.; Dennemarker, J.; Lohmüller, T.; Brömme, D.; Schüle, R.; Peters, C.; Reinheckel, T. *Eur. J. Cell Biol.* **2004**, *83*, 775.
4. Asaad, N.; Bethel, P. A.; Coulson, M. D.; Dawson, J. E.; Ford, S. J.; Gerhardt, S.; Grist, M.; Hamlin, G. A.; James, M. J.; Jones, E. V.; Karoutchi, G. I.; Kenny, P. W.; Morley, A. D.; Oldham, K.; Rankine, N.; Ryan, D.; Wells, S. L.; Wood, L.; Augustin, M.; Krapp, S.; Simader, H.; Steinbacher, S. *Bioorg. Med. Chem. Lett.*, 2009, 19, 4280.
5. Honig, B.; Nicholls, A. *Science* **1995**, *268*, 1144.
6. Young, T.; Abel, R.; Kim, B.; Berne, B. J.; Friesner, R. A. *Proc. Nat. Acad. Sci.* **2007**, *104*, 808.
7. Bogan, A. A.; Thorn, K. S. *J. Mol. Biol.* **1998**, *280*, 1.
8. DeLano, W. L. *Curr. Opin. Struct. Biol.* **2002**, *12*, 14.
9. Hajduk, P. J.; Huth, J. R.; Fesik, S. W. *J. Med. Chem.* **2005**, *48*, 2518.
10. Erlanson, D. A.; McDowell, R. S.; O'Brien, T. *J. Med. Chem.* **2004**, *47*, 3463.
11. Congreve, M.; Chessari, G.; Tisi, D.; Woodhead, A. J. *J. Med. Chem.* **2008**, *51*, 3661.
12. There are four protein molecules in the asymmetric unit of the crystal structure of the complex of Cathepsin L with **2**. The ranges for the H–H distance and angle between the NH vectors are 2.77 Å to 2.84 Å and 25° to 27°, respectively.
13. Abraham, M. H.; Duce, P. D.; Prior, D. V.; Barratt, D. G.; Morris, J. J.; Taylor, P. J. *J. Chem. Soc., Perkin Trans. 2* **1989**, 1355.
14. Kenny, P. W. *J. Chem. Soc., Perkin Trans. 2* **1994**, 199.
15. Jorgensen, W. L.; Pranata, J. *J. Am. Chem. Soc.* **1990**, *112*, 2008.
16. $pIC_{50} = -\log(IC_{50}/M)$.
17. Values of pIC_{50} for inhibition of Cathepsins L, L2, S, K and B were determined from dose dependent inhibition of cleavage of fluorogenic, AMC-tagged, peptide substrates. See also Ref. 18.
18. Hulkower, K. I.; Butler, C. C.; Linebaugh, B. E.; Klaus, J. L.; Keppler, D.; Giranda, V. L.; Sloane, B. F. *Eur. J. Biochem.* **2000**, *267*, 4165.
19. Gupta, S.; Singh, R. K.; Dastidar, S.; Ray, A. *Exp. Opin. Ther. Targets* **2008**, *12*, 291.
20. Diffraction data for compound **35** were collected at 100 K on beamline PX at the Swiss Light Source (SLS, Villigen, Switzerland). The structure was solved by molecular replacement and refined to a final resolution of 2.33 Å and R-factor of 25.0% using the CCP4 (Ref. 21) and Coot (Ref. 22) software packages. This structure has been deposited in the RSB (home.rcsb.org) Protein Data Bank (www.rcsb.org/pdb/home/home.do) with reference code 3HWN.
21. Collaborative Computational Project, Number 4; (http://www.ccp4.ac.uk) Acta Crystallogr. 1994, D50, 760.
22. Coot: http://www.ysbl.york.ac.uk/~emsley/coot.
23. Davis, A. M.; Teague, S. J. *Angew. Chem., Int. Ed.* **1999**, *38*, 736.